

A mechanism for how Cdr1/Nim1 kinase promotes mitotic entry by inhibiting Wee1

Hannah E. Opalko^a, Isha Nasa^{a,b}, Arminja N. Kettenbach^{a,b}, and James B. Moseley^{a,*}

^aDepartment of Biochemistry and Cell Biology, The Geisel School of Medicine at Dartmouth, Hanover, NH 03755;

^bNorris Cotton Cancer Center, The Geisel School of Medicine at Dartmouth, Lebanon, NH 03756

ABSTRACT To enter into mitosis, cells must shut off the cell cycle inhibitor Wee1. SAD family protein kinases regulate Wee1 signaling in yeast and humans. In *Schizosaccharomyces pombe*, two SAD kinases (Cdr1/Nim1 and Cdr2) act as upstream inhibitors of Wee1. Previous studies found that *S. pombe* Cdr1/Nim1 directly phosphorylates and inhibits Wee1 in vitro, but different results were obtained for budding yeast and human SAD kinases. Without a full understanding of Cdr1 action on Wee1, it has been difficult to assess the in vivo relevance and conservation of this mechanism. Here, we show that both Cdr1 and Cdr2 promote Wee1 phosphorylation in cells, but only Cdr1 inhibits Wee1 kinase activity. Inhibition occurs when Cdr1 phosphorylates a cluster of serine residues linking α -helices G and H of the Wee1 kinase domain. This region is highly divergent among different Wee1 proteins, consistent with distinct regulatory mechanisms. A *wee(4A)* mutant that impairs phosphorylation by Cdr1 delays mitotic entry and causes elongated cells. By disrupting and retargeting Cdr1 localization, we show that Cdr1 inhibition of Wee1 occurs in cells at cortical nodes formed by Cdr2. On the basis of our results, we propose a two-step model for inhibition of Wee1 by Cdr1 and Cdr2 at nodes.

Monitoring Editor

Daniel J. Lew
Duke University

Received: Aug 9, 2019

Revised: Oct 8, 2019

Accepted: Oct 16, 2019

INTRODUCTION

Eukaryotic cells enter into mitosis due to regulated activation of Cdk1. During interphase, Cdk1 is kept inactive by the protein kinase Wee1, which phosphorylates Cdk1-Y15 to inhibit Cdk1 activity (Nurse, 1975; Gould and Nurse, 1989; Featherstone and Russell, 1991; Lundgren *et al.*, 1991; Parker *et al.*, 1992; Coleman *et al.*, 1993). As cells enter mitosis, this inhibitory phosphorylation is removed by the phosphatase Cdc25 to activate Cdk1 (Russell and Nurse, 1986; Dunphy and Kumagai, 1991; Gautier *et al.*, 1991; Kumagai and Dunphy, 1991; Strausfeld *et al.*, 1991). To enter mitosis, cells must inhibit Wee1, thereby relieving the “brake” on Cdk1. This mechanism acts as a bistable switch due to feedback in which Cdk1 inhibits Wee1 and activates Cdc25 (Mueller *et al.*, 1995; Pomerening *et al.*, 2003; Sha *et al.*, 2003; Harvey *et al.*, 2005; Kim

and Ferrell, 2007). Many upstream mechanisms that regulate Wee1 are not well defined. The fission yeast *Schizosaccharomyces pombe* has served as a long-standing model system for this conserved regulatory module. These rod-shaped cells enter into mitosis and divide at a reproducible size due to the activities of Wee1, Cdc25, and other Cdk1 regulators. Decades of work identified key factors upstream of Cdk1, but it has remained a challenge to place these factors into defined pathways and to understand their biochemical mechanisms.

Genetic screens in fission yeast defined two SAD-family (synapses of the amphid defective) protein kinases, Cdr1/Nim1 and Cdr2, as upstream inhibitors of Wee1. Both *cdr1* and *cdr2* mutants divide at a larger size than wild-type cells due to uninhibited Wee1 (Russell and Nurse, 1987; Young and Fantes, 1987; Breeding *et al.*, 1998; Kanoh and Russell, 1998). The cell size defects of *cdr1* and *cdr2* mutants are nonadditive (Feilotter *et al.*, 1991; Martin and Berthelot-Grosjean, 2009; Moseley *et al.*, 2009), suggesting redundant or related inhibitory mechanisms. Wee1 becomes increasingly phosphorylated as cells grow during G2 (Lucena *et al.*, 2017). This phosphorylation is reduced in *cdr1Δ* and *cdr2Δ* mutants (Allard *et al.*, 2018), consistent with increasing inhibition by Cdr1-Cdr2. Cdr2 appears to act primarily through localization of Wee1. Cdr2 forms cortical node structures in the cell middle and recruits both Cdr1 and Wee1 to these sites (Morrell *et al.*, 2004; Martin and Berthelot-Grosjean, 2009; Moseley *et al.*, 2009; Allard *et al.*, 2018).

This article was published online ahead of print in MBoC in Press (<http://www.molbiolcell.org/cgi/doi/10.1091/mbc.E19-08-0430>) on October 23, 2019.

*Address correspondence to: James B. Moseley (james.b.moseley@dartmouth.edu).

Abbreviations used: GBP, GFP-binding peptide; PBS, phosphate-buffered saline; SAD, synapses of the amphid defective; WCE, whole-cell extracts.

© 2019 Opalko *et al.* This article is distributed by The American Society for Cell Biology under license from the author(s). Two months after publication it is available to the public under an Attribution–Noncommercial–Share Alike 3.0 Unported Creative Commons License (<http://creativecommons.org/licenses/by-nc-sa/3.0>).

“ASCB®,” “The American Society for Cell Biology®,” and “Molecular Biology of the Cell®” are registered trademarks of The American Society for Cell Biology.

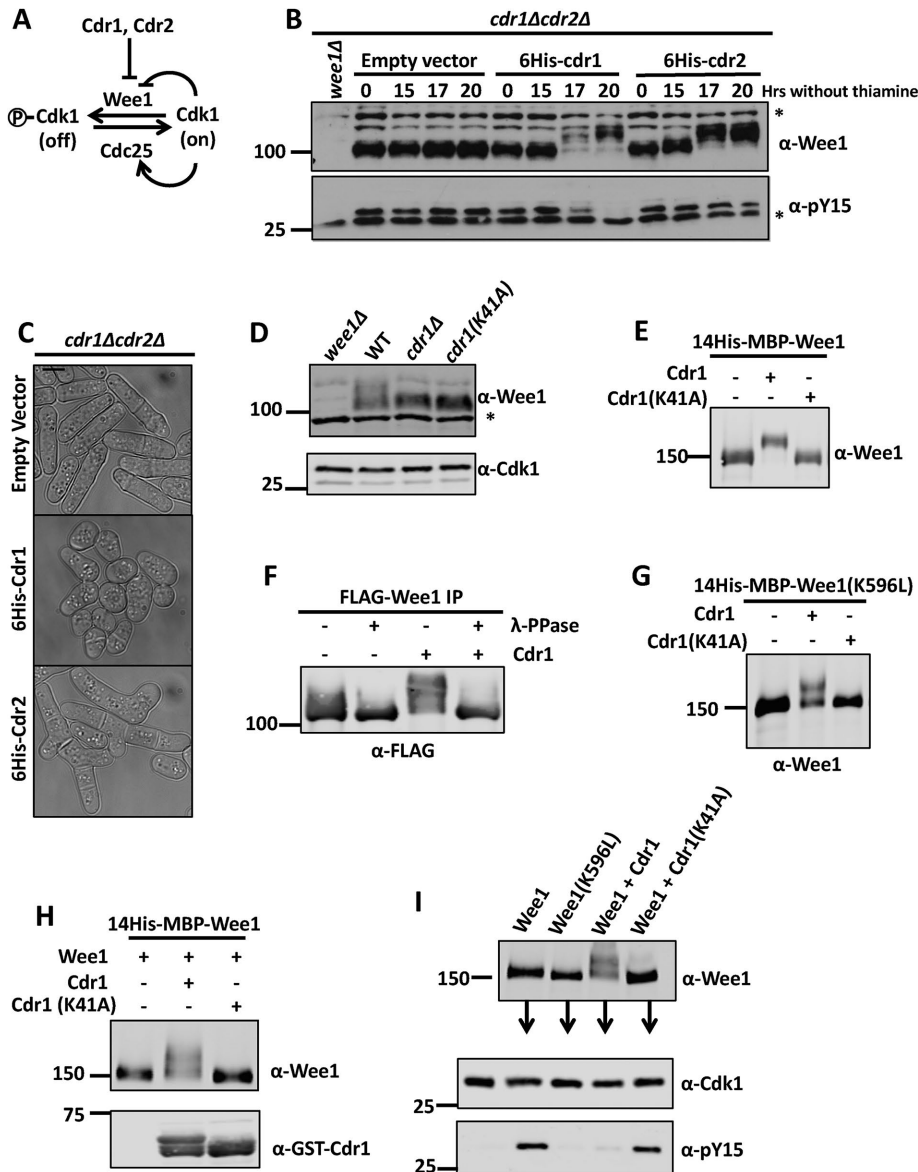


FIGURE 1: Cdr1 phosphorylates and inhibits Wee1. (A) Schematic of pathway. (B) Whole-cell extracts (WCE) were separated by SDS–PAGE and Western blotted against endogenous Wee1. Cdk1-pY15 levels were monitored for Wee1 activity; asterisks mark background bands. (C) Differential interference contrast (DIC) images of *cdr1Δcdr2Δ* cells with overexpression plasmids. Scale bar, 5 μ m. (D) WCE were separated by SDS–PAGE and blotted against endogenous Wee1. Cdk1 is used as a loading control; the asterisk denotes background band. (E) Cdr1 phosphorylates Wee1 in Sf9 cells. Wee1 was coexpressed with Cdr1 or Cdr1(K41A) in Sf9 cells. (F) Cdr1-dependent band shift is due to phosphorylation of Wee1. Wee1 was expressed alone or coexpressed with Cdr1, immunoprecipitated, and treated with λ -phosphatase. (G) Coexpression of Wee1(K596L) with Cdr1/Cdr1(K41A) in Sf9 cells. (H) Cdr1 phosphorylates Wee1 directly in vitro. GST-Cdr1(1-354) was expressed and purified from bacteria and mixed with ATP and purified 14His-MBP-Wee1. (I) Cdr1-dependent phosphorylation of Wee1 inhibits Wee1 kinase activity. Wee1 was phosphorylated by Cdr1 as in (H) and then incubated with Cdk1-Cdc13 immunoprecipitated from *S. pombe*. Cdk1-pY15 was used to monitor Wee1 kinase activity.

Cdr1/Nim1 appears to be the key protein that directly regulates Wee1 activity. In vitro, Cdr1 phosphorylates and inhibits Wee1 kinase activity (Coleman *et al.*, 1993; Parker *et al.*, 1993; Wu and Russell, 1993). However, key questions have remained open regarding this mechanism. The in vivo relevance of Cdr1 phosphorylating Wee1 has not been tested because direct phosphorylation sites have been unknown. In addition, different results have been

obtained for regulation of Wee1 by SAD family kinases in budding yeast and humans (Kellogg, 2003; Lu *et al.*, 2004; Sakchaisri *et al.*, 2004; Keaton and Lew, 2006). In this study, we investigated how Cdr1 inhibits Wee1. Our combined results lead to a mechanistic model for Wee1 regulation by SAD kinases in fission yeast.

RESULTS AND DISCUSSION

Cdr1 phosphorylates and inhibits Wee1

Cdr1 and Cdr2 act as upstream inhibitors of Wee1 (Figure 1A). To test their mechanisms, we overexpressed Cdr1, Cdr2, or the empty vector in *cdr1Δcdr2Δ* cells. We monitored Wee1 phosphorylation by SDS–PAGE band shift (Lucena *et al.*, 2017; Allard *et al.*, 2018) and Wee1 activity by Cdk1-pY15 levels (Figure 1B). Cdr1 overexpression induced hyperphosphorylation of Wee1 and loss of Cdk1-pY15, indicating inhibition of Wee1 kinase activity, consistent with previous work (Coleman *et al.*, 1993; Parker *et al.*, 1993; Wu and Russell, 1993). In contrast, Cdr2 overexpression induced hyperphosphorylation of Wee1 but no change in Cdk1-pY15. Thus, both Cdr1 and Cdr2 induce phosphorylation of Wee1, but the regulatory output of these two kinases is distinct. Consistent with these biochemical results, only overexpression of Cdr1 but not of Cdr2 resulted in reduced cell size in *cdr1Δcdr2Δ* cells (Figure 1C), consistent with previous results in wild-type cells (Russell and Nurse, 1987; Breeding *et al.*, 1998). Phosphorylation of Wee1 in fission yeast cells was reduced in the catalytically inactive mutant *cdr1(K41A)* (Figure 1D), similar to *cdr1Δ* cells (Allard *et al.*, 2018). Given the role of Cdr1 in regulating Wee1 kinase activity, along with open questions regarding its underlying mechanism, we investigated this pathway further.

Previous studies found that Cdr1 can directly phosphorylate and inhibit Wee1 kinase activity in vitro (Coleman *et al.*, 1993; Parker *et al.*, 1993; Wu and Russell, 1993). However, in budding yeast, the Cdr1-like kinase Hsl1 does not phosphorylate or inhibit the Wee1-like kinase Swe1 (Kellogg, 2003; Sakchaisri *et al.*, 2004; Keaton and Lew, 2006). These conflicting results indicate that a more detailed analysis of the mechanism for Cdr1-Wee1 regulation is needed. Consistent with previous work (Coleman *et al.*, 1993; Parker *et al.*, 1993; Wu and Russell, 1993), coexpression of Wee1 and active Cdr1 in Sf9 insect cells caused a phosphorylation-dependent shift in the SDS–PAGE migration of Wee1 (Figure 1, E and F). Phosphorylation of Wee1 was not induced by coexpression with catalytically inactive *cdr1(K41A)* (Figure 1E). Further, the shift was not due to autophosphorylation because we observed a similar result using the inactive

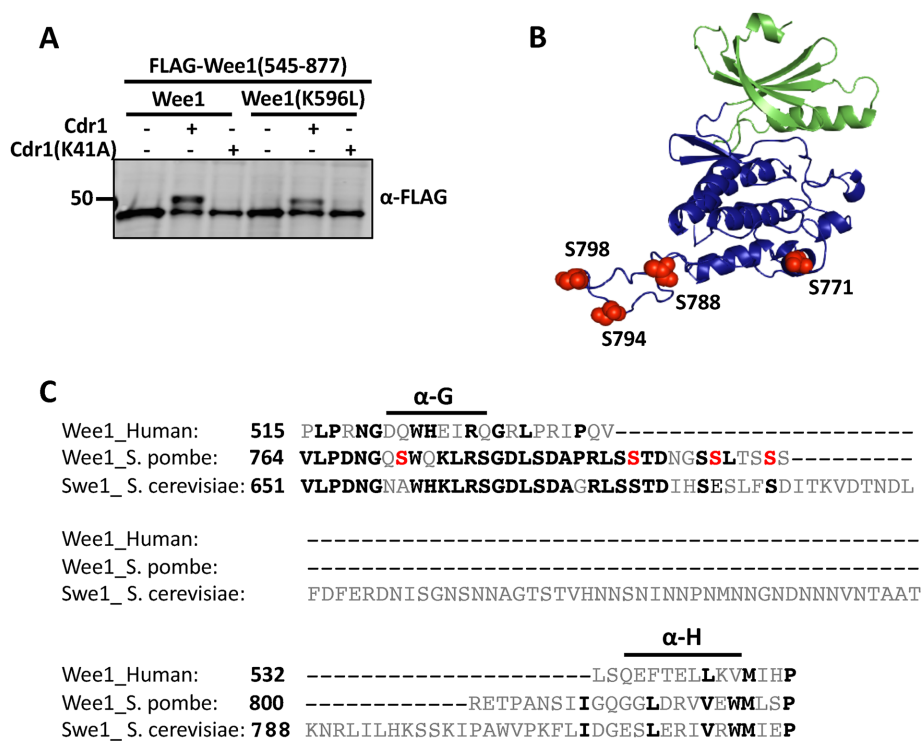


FIGURE 2: Identification of Cdr1-dependent phosphorylation sites on Wee1. (A) Cdr1 phosphorylates the Wee1 kinase domain. The 10His-Cdr1 or 10His-Cdr1(K41A) was coexpressed in Sf9 cells with either FLAG-Wee1(545–877) or FLAG-Wee1(545–877; K596L). (B) Model of *S. pombe* Wee1 kinase domain threaded into human Wee1 from SWISS-MODEL. Green region indicates the N-terminal lobe; blue highlights the C-terminal lobe. Phosphorylated residues in the extended loop are marked in red. (C) Sequence alignment of human, *S. pombe*, and *S. cerevisiae* Wee1. Red serines are phosphorylated by Cdr1. Black amino acids are conserved.

mutant *wee1(K596L)* (Figure 1G). As a more direct test, we performed *in vitro* kinase assays with purified proteins (Supplemental Figure S1, A–E) including the active construct Cdr1(1–354), which was expressed and purified from bacteria. Cdr1 directly phosphorylated Wee1, but Cdr1(K41A) did not (Figure 1H). We performed two-step *in vitro* kinase assays to test the effects of this phosphorylation on Wee1 activity. Wee1 that was phosphorylated by Cdr1 did not phosphorylate its substrate Cdk1-Y15, whereas Wee1 retained activity after incubation with Cdr1(K41A) (Figure 1I). Taken together, our results show that Cdr1 phosphorylates Wee1 in fission yeast cells, insect cells, and *in vitro*. Our findings confirm and extend past work showing that Cdr1 directly phosphorylates Wee1, and this modification inhibits Wee1 kinase activity (Coleman *et al.*, 1993; Parker *et al.*, 1993; Wu and Russell, 1993).

Cdr1-dependent phosphorylation sites on Wee1

Next, we sought to identify the sites on Wee1 that are targeted by Cdr1 for inhibitory phosphorylation. We used liquid chromatography with tandem mass spectrometry (LC-MS/MS) to map Wee1 phosphorylation sites from three independent experiments (Supplemental Table S2). First, we purified Wee1 from insect cells following its expression either alone or in combination with Cdr1. We identified sites that were phosphorylated specifically upon coexpression with Cdr1. Second, we performed a similar experiment with the inactive mutant Wee1(K596L) to ensure that identified sites were not due to autophosphorylation. Third, we performed *in vitro* kinase assays by mixing purified Wee1 or inactive Wee1(K596L) with either active Cdr1 or inactive Cdr1(K41A) and then mapped Wee1

phosphorylation sites specifically induced by active Cdr1. A number of phosphorylation sites were identified in multiple experiments throughout the Wee1 sequence (Supplemental Figure S2B). We focused primarily on sites in the kinase domain because Cdr1 regulates Wee1 kinase activity and phosphorylates the kinase domain alone (Figure 2A; Supplemental Figure S2A) (Coleman *et al.*, 1993; Parker *et al.*, 1993).

To pinpoint which of these phosphorylation sites mediate inhibition of Wee1 by Cdr1 in cells, we generated a panel of mutants in which different phosphorylated residues were changed to alanine, thereby preventing phosphorylation. We reasoned that a non-phosphorylatable Wee1 mutant would be hyperactive, leading to an elongated cell length at division similar to *cdr1Δ* cells. These constructs were integrated into the genome and expressed by the *wee1* promoter as the sole copy in these cells. By analyzing combinations of mutations, we determined that some mutations (e.g., S21A and S822A) had no effect on cell size, while others (e.g., S781A) caused a loss-of-function *wee* phenotype (Supplemental Figure S2C and Supplemental Table S1). Importantly, we generated one mutant that mimicked the *cdr1Δ* phenotype. We named this mutant *wee1(4A)* because it prevents phosphorylation at four sites: S771, S788, S794, and S798.

The phosphorylation sites mutated in *wee1(4A)* are clustered within the C-lobe of the kinase domain and have interesting regulatory potential. Using sequence alignments and structural modeling, this cluster falls mostly within a loop that connects α-helices G and H of the Wee1 kinase domain (Figure 2, B and C) (Squire *et al.*, 2005). This loop is extended in *S. pombe* Wee1 as compared with human Wee1, so the sites are not obviously present in the human polypeptide sequence. Interestingly, this loop is dramatically extended and asparagine rich in the *Saccharomyces cerevisiae* Swe1 sequence, and therefore the conserved sites may not be subject to a related regulatory mechanism (Figure 2C). Several eukaryotic protein kinases have extended loops connecting α-G and α-H within the GHI subdomain (Hanks and Hunter, 1995; Scheeff and Bourne, 2005). This subdomain acts as a substrate docking site and connects to the activation segment to regulate catalytic activity (Deminoff *et al.*, 2009; Taylor *et al.*, 2012). Thus, posttranslational modifications in this region have the potential to regulate kinase activity.

wee1(4A) prevents regulation by Cdr1

We performed a series of *in vivo* experiments to test key predictions for the *wee1(4A)* mutant. First, if Cdr1 functions by phosphorylating these residues, then cellular phosphorylation of Wee1 should be reduced in the *wee1(4A)* mutant. Consistent with this model, *wee1(4A)* phosphorylation was reduced when compared with wild type, and its phosphorylation was not altered by *cdr1Δ* or *cdr2Δ* (Figure 3A). Second, if both *cdr1Δ* and *wee1(4A)* mutants are elongated at division due to the same pathway, then combining these two mutations should not generate additive or synthetic defects. Indeed, *cdr1Δ wee1(4A)* cells divided at the same size as *cdr1Δ* cells

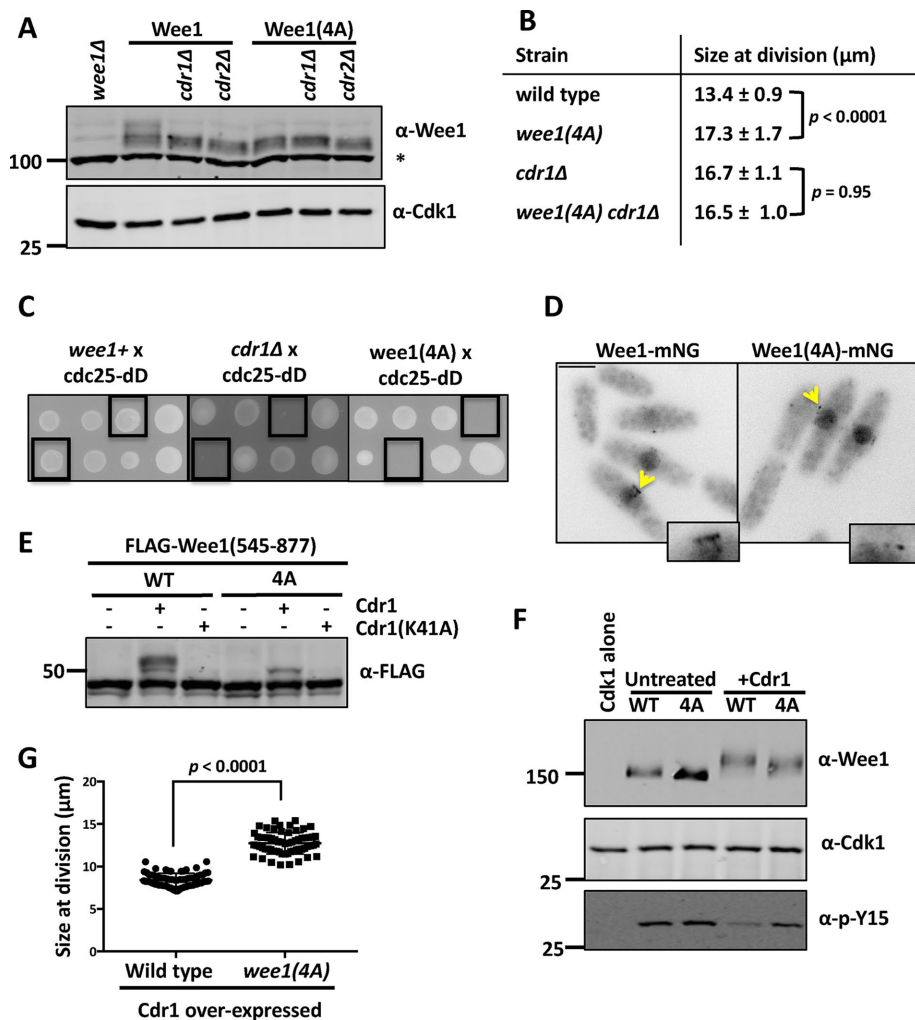


FIGURE 3: Phenotypes of phosphorylation-resistant *wee1(4A)* mutant. (A) WCE samples were separated by SDS-PAGE and blotted to detect Wee1. Cdk1 is used as a loading control; the asterisk marks background band. (B) Cell size measurements of the indicated strains. Values are mean ± SD for $n > 50$ each strain; the p value for one-way ANOVA shown for wild-type vs. *wee1(4A)*, and for *cdr1Δ* vs. *wee1(4A) cdr1Δ*. (C) Both *wee1(4A)* and *cdr1Δ* are synthetically lethal with *cdc25-dD*. Black boxes indicate double mutants from tetrad analysis. (D) Localization to nucleus and cortical nodes is unaffected in the *wee1(4A)* mutant. Middle focal plane images. Scale bar, 5 μm. Boxes are enlarged images of nodes denoted by a yellow arrow. (E) 4A mutation prevents Cdr1-dependent phosphorylation of the Wee1 kinase domain. Coexpression of wild type or Wee1(4A) with Cdr1/Cdr1(K41A). (F) Wee1(4A) has impaired Cdr1 inhibition. The Wee1 kinase activity was tested as in Figure 1I. (G) Cell size at division for the indicated strains, showing mean and SD for $n > 50$ cells each; the p value was from unpaired T test.

(Figure 3B and Supplemental Table S1). Third, *wee1(4A)* mutations should be additive or synthetic with mutations in *cdc25*. Past work has shown that *cdr1* mutations are synthetically lethal with *cdc25* mutant alleles (Young and Fantes, 1987). Both *wee1(4A)* and *cdr1Δ* were synthetically lethal with *cdc25-dD* (Figure 3C). These combined experiments show that *wee1(4A)* recapitulates the *cdr1Δ* phenotype and prevents Wee1 phosphorylation in cells.

Next, we addressed potential mechanisms that could explain the phenotype of *wee1(4A)*. We confirmed that *wee1(4A)* protein level does not increase and still localizes to cortical nodes (Figure 3, A and D). However, Cdr1 was unable to induce hyperphosphorylation of the *wee1(4A)* kinase domain in insect cells (Figure 3E). In two-step in vitro kinase assays, Cdr1 readily inhibited Wee1 but not *wee1(4A)* (Figure 3F). Unlike wild-type Wee1, the *wee1(4A)* mutant

still phosphorylated Cdk1-pY15 after treatment with Cdr1. These results indicate that the primary defect of the *wee1(4A)* mutant is loss of inhibition by Cdr1. Accordingly, the size of *wee1(4A)* cells was largely (but not entirely) insensitive to Cdr1 overexpression (Figure 3G). Taken together, our results show that phosphorylation of these four residues by Cdr1 inhibits Wee1 activity. We note that the 4A mutation does not completely abolish Wee1 phosphorylation and regulation by Cdr1 in vitro, and Cdr1 phosphorylates additional residues both within and beyond the Wee1 kinase domain. Thus, *wee1(4A)* explains regulation by Cdr1 in vitro and in vivo, but we do not rule out a role for phosphorylation of additional residues in Cdr1-Wee1 regulation.

Wee1 has also been shown to be phosphorylated and inhibited by Cdk1 in budding yeast, humans, and other systems (Mueller *et al.*, 1995; Harvey *et al.*, 2005). This feedback sharpens the ultrasensitive nature of Cdk1 activation for mitotic entry (Pomerening *et al.*, 2003; Sha *et al.*, 2003; Kim and Ferrell, 2007). Whether this feedback occurs in fission yeast and its regulation by Cdr1 has not been tested. We used the analogue-sensitive Cdk1-asM17 allele (Aoi *et al.*, 2014), which can use bio-orthogonal 6-Bn-ATPγS to thiophosphorylate direct substrates (Allen *et al.*, 2007; Hertz *et al.*, 2010). We confirmed that *S. pombe* Cdk1-asM17 directly thiophosphorylates Wee1 and Wee1(K596L) (Figure 4A). Thus, Cdk1 phosphorylates Wee1 in fission yeast, similar to those of other systems. Next, we found that Wee1 phosphorylation by Cdr1 did not impair the level of thiophosphorylation by Cdk1-asM17 (Figure 4B). We conclude that Cdr1 phosphorylation of Wee1 does not block subsequent phosphorylation by Cdk1.

Spatial control of Cdr1-Wee1 signaling in cells

Cdr1 and Wee1 both localize to cortical nodes in the cell middle (Martin and Berthelot-Grosjean, 2009; Moseley *et al.*, 2009; Allard *et al.*, 2018). These nodes are formed by Cdr2 oligomers that are required for Cdr1 and Wee1 recruitment (Martin and Berthelot-Grosjean, 2009; Moseley *et al.*, 2009; Allard *et al.*, 2018). We previously identified a mutant *cdr1(Δ460-482)* that fails to localize to nodes and results in elongated cell size at division like *cdr1Δ* (Figure 5A) (Opalko and Moseley, 2017). We tested the effects of artificially recruiting mEGFP-*cdr1(Δ460-482)* back to nodes using *cdr2*-GFP-binding peptide (GBP)-mCherry, which contains the GBP. In this system, mEGFP-*cdr1(Δ460-482)* colocalized with *cdr2*-GBP-mCherry at nodes (Figure 5B). More importantly, recruitment back to nodes had strong effects on cell size and Wee1 phosphorylation (Figure 5, C and D, and Supplemental Table S1). In the *cdr1(Δ460-482)* mutant, Wee1 was not hyperphosphorylated and cells divided at an increased size, similar to that of *cdr1Δ*. However, recruitment of

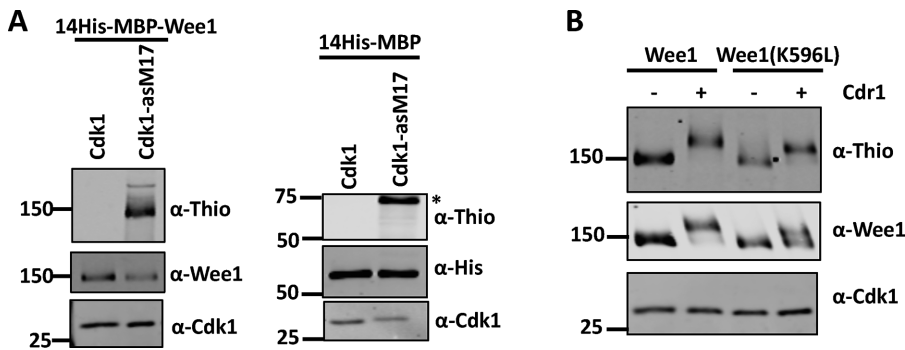


FIGURE 4: Cdk1 phosphorylation of Wee1 is not blocked by Cdr1. (A) Cdk1 phosphorylates Wee1 in vitro. Left: Wild-type Cdk1 or Cdk1-asM17 was immunoprecipitated and incubated with purified 14His-MBP-Wee1. These in vitro assays used bio-orthogonal 6-Bn-ATP γ S, which can only be utilized by Cdk1-asM17 to thiophosphorylate direct substrates. Right: Cdk1-asM17 does not phosphorylate 14His-MBP. The asterisk denotes background band. (B) Cdk1-asM17 thiophosphorylates both Wee1 and Wee1(K596L). This activity is not blocked by prior phosphorylation of Wee1 constructs by Cdr1.

mEGFP-cdr1(Δ 460–482) back to nodes by cdr2-GFP-mCherry caused Wee1 to be even more hyperphosphorylated than in wild-type cells. A similar effect was seen using full-length mEGFP-cdr1. Along with enhanced Wee1 hyperphosphorylation, these cells divided at a smaller size than wild-type cells. These results show that Cdr1 localization to nodes is a limiting factor for phosphorylation of Wee1 and cell size at division. Further, they demonstrate that cdr1(Δ 460–482) retains activity but can phosphorylate Wee1 only at nodes, strongly supporting a model where inhibitory phosphorylation of Wee1 occurs at nodes.

Our results combined with past work suggest a two-step mechanism for regulation of a Wee1 molecule at nodes (Figure 5E). Wee1 localizes to nodes in transient bursts that last between 5 and 15 s (Allard *et al.*, 2018). This localization requires Wee1's noncatalytic N-terminus, which can be phosphorylated by Cdr2 (Kanoh and Russell, 1998; Allard *et al.*, 2018). In kinase-dead *cdr2* mutants, Wee1 localizes to nodes in extremely short bursts (<2 s) (Allard *et al.*, 2018). As the first step toward inhibition, we propose that Cdr2 phosphorylates the Wee1 N-terminus to slow the off-rate for Wee1 release, thereby "trapping" Wee1 in the node. In the second step, Cdr1 within the node can then phosphorylate the Wee1 kinase domain to inhibit catalytic activity of this molecule through the mechanism described in this study. These two steps are consistent with many past results and show how these two related kinases control distinct aspects of a shared inhibitory mechanism. An open question going forward is why this reaction needs to occur at nodes. It is possible that nodes simply increase the local concentration of Cdr1 and Wee1. Indeed, both Cdr1 and Wee1 are expressed at low levels, which could preclude an efficient interaction in the cytoplasm. This possibility is supported by the finding that Cdr1 overexpression bypasses the need for Cdr2, leading to Wee1 hyperphosphorylation, inhibition of Wee1, and reduced cell size (Figure 1, B and C). An alternative possibility is that the structure of a node promotes efficient phosphorylation of Wee1, for example, by promoting a more active conformation of Cdr1. These and other possibilities are not mutually exclusive, and additional work on this system may reveal general principles for the emerging theme of signal transduction in cortical clusters.

In conclusion, we have answered long-standing questions regarding how Cdr1/Nim1 inhibits Wee1 in fission yeast cells. Cdr1 inhibits the kinase activity of Wee1 by directly phosphorylating a cluster of residues connecting α -helices G and H. The sequence of

this region is evolutionarily divergent, likely explaining why Cdr1-like kinases may not act directly on Wee1 in some other species. However, the functional role of this region within kinase domains suggests that other kinases with insertions at the GHI subdomain may be regulated by mechanisms similar to the one we describe here. Phosphorylation of these residues in Wee1 explains the cell size defects of *cdr1* Δ mutants and likely represent the functional output of the well-studied Pom1-Cdr2-Cdr1-Wee1 pathway (Martin and Berthelot-Grosjean, 2009; Moseley *et al.*, 2009; Pan *et al.*, 2014; Allard *et al.*, 2018, 2019; Gerganova *et al.*, 2019). Efficient signaling in this pathway requires organization within oligomeric clustered structures at the cell cortex. Given the critical role of these structures in relaying cell size information to the core cell cycle machinery, additional insight

into the underlying mechanisms will have implications for cell size control. Molecular clusters are a feature of many other signal transduction pathways, so the Cdr2/Cdr1/Wee1 network will also serve as a model for broader mechanistic studies of signal transduction.

MATERIALS AND METHODS

Yeast strains and growth

Standard *S. pombe* media and methods were used (Moreno *et al.*, 1991). Strains and plasmids used in this study are listed in Supplemental Table S1. The Sf9 constructs were cloned via restriction digest into Fastbac vector (Thermo Fisher Scientific). Mutations in the Wee1 or Cdr1 gene were made by Gibson assembly (QuantaBio), or by site-directed mutagenesis by Quikchange (Stratagene). Wee1 was expressed in a pJK148 plasmid containing wild-type Wee1 along with 1000 base pairs each of the Wee1 promoter and terminator. To introduce *wee1* mutations into cells, we deleted one copy of *wee1+* from a wild-type diploid strain (JM5334) using PCR-based homologous recombination to generate the heterozygous diploid strain JM5337. Mutant *wee1* alleles in pJK148-based plasmids were then transformed into the *leu1* locus. Diploid cells were then sporulated, and the resulting spores were separated via tetrad dissection. Colonies that grew on *leu-* plates and were G418 resistant were verified by colony PCR and by Western blot analysis.

To test for synthetic lethality with *cdc25* mutants, we used a *cdc25-degron-DAMP::hygro* strain. The *wee1+* (JM5578), *wee1(4A)* (JM5709), and *cdr1* $\Delta::kanMX6$ (JM483) were crossed to *cdc25-degron DAMP::hygro* (JM5886/JM5887). A full plate of tetrads was analyzed (9–10 tetrads). Crosses with the *wee1(4A)* yielded a synthetic lethality with *cdc25-degron-DAMP(dD)* both with and without a wild-type copy of Wee1 at the endogenous locus. When *cdc25-dD* was crossed to a *cdr1* Δ with the *wee1* $\Delta::kanMX6$ *leu1(Pwee1-wee1-Twee1)* background, *cdr1* Δ cells were also synthetically lethal with *cdc25-degron DAMP* both with and without a wild-type copy of Wee1 at the endogenous locus. To look specifically at the genetic interaction between Cdr1 and Cdc25 with one copy of wild-type Wee1 present, a *cdr1* $\Delta::kanMX6$ strain in a wild-type background was crossed to *cdc25-dD*. For mEGFP-Cdr1(Δ 460–482), Cdr1 was mutated in a pJK148 vector containing 970 base pairs of Cdr1 promoter, mEGFP-Cdr1 and 300 base pairs of Cdr1 terminator. Each vector was then integrated into the *leu1* locus in *cdr1* $\Delta::kanMX6$ *leu1-32*.

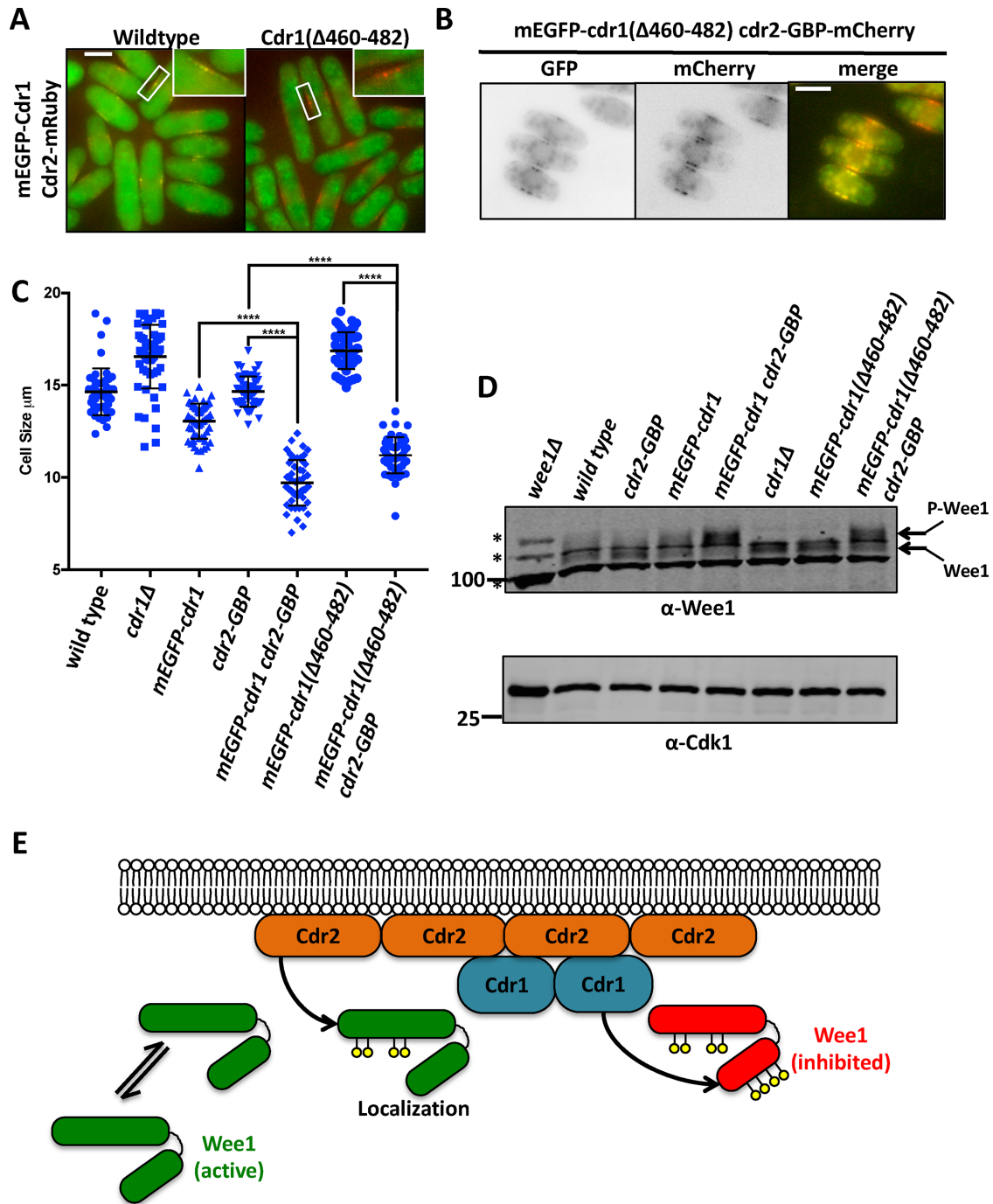


FIGURE 5: Wee1 inhibition occurs at nodes. (A) mEGFP-tagged Cdr1 or Cdr1(Δ 460-482) with Cdr2-mRuby. Scale bar, 5 μm . (B) Colocalization of mEGFP-*cdr1*(Δ 460-482) Cdr2-GBP-mCherry. Scale bar, 5 μm . (C) Tethering Cdr1(Δ 460-482) to nodes rescues size defect. Cell size measurements of indicated strains. Line marks mean; error bars mark SD, $n > 50$ for each strain. A one-way ANOVA was used for statistical comparisons. **** $p < 0.0001$. (D) Cdr1 localization dictates Wee1 phosphorylation state. WCEs were separated by SDS-PAGE. Note upper, hyperphosphorylated band for Wee1 upon node targeting of Cdr1. Cdk1 was used as a loading control; the asterisk marks background band. (E) Model for two-step inhibition of a Wee1 molecule at a node.

For Cdr1 or Cdr2 overexpression, pREP3x plasmids were transformed into *cdr1::kanMX6 cdr2Δ::ura4 ULA-* (JM2070) cells and grown in Edinburgh minimal media (EMM) $-\text{leu} +\text{thiamine}$. Cells were then washed vigorously and resuspended in EMM $-\text{leu}$ to induce expression of Cdr1 or Cdr2, starting at time point 0. For the experiment in Figure 3G, cells were grown at 32°C in EMM4S lacking thiamine for 19 h before analyzing. GFP-Cdr1 was overexpressed

to the same level in both strains as verified by Western blot using α -GFP antibodies.

Sf9 cell coexpression and Wee1 purification

Sf9 cells were grown in Grace's media supplemented (Life Technologies) with 10% heat inactivated fetal bovine serum, 10 $\mu\text{g/ml}$ gentamicin, and 0.25 $\mu\text{g/ml}$ amphotericin B at 27°C. Constructs

were expressed in Sf9 cells using the Bac-to-Bac Baculovirus expression system (Thermo Fisher Scientific). Wee1 constructs were coexpressed with Cdr1/Cdr1(K41A) for 3 d. Cells were resuspended in SDS–PAGE sample buffer (65 mM Tris, pH 6.8, 3% SDS, 10% glycerol, 10% 2-mercaptoethanol, 50 mM sodium fluoride, 50 mM β -glycerophosphate, 1 mM sodium orthovanadate, complete EDTA-free protease inhibitor tablet [Pierce]) and boiled for 5 min, and the resulting lysates were separated by SDS–PAGE.

For purification of Wee1 from Sf9 cells, 14His-3C-MBP-Wee1 was expressed in Sf9 cells for 3 d. Cells were then harvested and resuspended in lysis buffer (50 mM Tris, pH 7.5, 150 mM NaCl, 75 mM sodium fluoride, 75 mM β -glycerophosphate, 1 mM phenylmethylsulfonyl fluoride [PMSF], 10 mM imidazole, pH 8, complete EDTA-free protease inhibitor tablet [Pierce]). Cells were lysed by French press. Triton X-100 was added to a final concentration of 1%, and glycerol was added to a concentration of 0.5%. Lysates were clarified by centrifuging at 15,000 rpm for 15 min at 4°C. Lysates were then added to TALON (TaKaRa) resin and incubated for 1 h at 4°C. The resin was then washed with wash buffer (50 mM Tris, pH 7.5, 500 mM NaCl, 75 mM sodium fluoride, 75 mM β -glycerophosphate, 20 mM imidazole, pH 8). Wee1 was then eluted using 500 mM imidazole pH 8. For purification and mass spectrometry, Wee1 was purified using the MBP tag due to coexpression with 10His-Cdr1. The approach was similar as above, except for the use of an amylose resin (New England Biolabs). Wee1 was then resuspended in elution buffer (1% SDS, 15% glycerol, 50 mM Tris, pH 8.7, 150 mM NaCl) and boiled for 5 min. The sample was reduced and alkylated prior to separation by SDS–PAGE.

Lambda phosphatase

For lambda phosphatase treatment, FLAG-Wee1 was coexpressed with Cdr1-MBP-14His for 3 d. Cells were harvested and lysed in lysis buffer (20 mM HEPES, pH 7.4, 1 mM EDTA, 300 mM NaCl, 0.2% Triton X-100, complete EDTA-free protease inhibitor tablet [Pierce], 75 mM sodium fluoride, 75 mM β -glycerophosphate, 1 mM sodium orthovanadate, 1 mM PMSF) by repeated freeze–thaw cycles. Lysates were centrifuged at 15,000 rpm at 4°C for 15 min. Clarified lysates were incubated with FLAG M2 magnetic beads (Sigma) for 1 h. Beads were then vigorously washed in lysis buffer lacking phosphatase inhibitors. Samples were split and treated with 800 U of lambda phosphatase (New England Biolabs) or mock treated at 30°C for 1 h.

In vitro kinase assay and Western blots

GST-Cdr1(1-354) and GST-Cdr1(1-354)(K41A) were expressed in BL21 *Escherichia coli* at 16°C. For these assays, Cdr1 was always freshly purified on the same day that it would be used. Cells were lysed in lysis buffer (1 \times phosphate-buffered saline [PBS], 300 mM NaCl, 1 mM dithiothreitol [DTT], 75 mM sodium fluoride, 75 mM β -glycerophosphate, 1 mM PMSF) by French press. Triton X-100 was added to a final concentration of 1% and glycerol to a concentration of 0.5%. Lysates were then centrifuged at 15,000 rpm for 20 min at 4°C. Clarified lysates were then incubated on glutathione-agarose (Sigma) for 1 h at 4°C. Agarose resin was then washed with wash buffer (1 \times PBS, 500 mM NaCl, 1 mM DTT, 75 mM sodium fluoride, 75 mM β -glycerophosphate) followed by 50 mM Tris, pH 7.5, 150 mM NaCl. GST-Cdr1 was maintained on glutathione-agarose resin for in vitro kinase reactions. Briefly, 0.3 μ g of purified 14His-3C-MBP-Wee1 was incubated with ~5–10 μ g of GST-Cdr1 in kinase buffer (50 mM Tris, pH 7.5, 10 mM MgCl₂ 1 mM DTT, 2 mM ATP, 3 μ M okadaic acid, 20 mM glutathione, pH 8) shaking for

1 h. To test Wee1 ability to phosphorylate Cdk1, 0.1 μ g Wee1 was incubated with Cdr1 for 10 min. Then reactions were spun down and soluble Wee1 was then added to Cdk1-Cdc13 complexes for 15 min. Cdk1-Cdc13 was immunoprecipitated from the fission yeast strain, *cdc13-FLAG wee1-50 mik1 Δ ::ura4+* after growth at the nonpermissive temperature for 3 h. Cdc13-FLAG was then immunoprecipitated as described above.

For the thiophosphate ester in vitro kinase assay, following the in vitro kinase assay with Cdr1 as described above, ATP- γ S (Axxora BLG-B072-05) was added to each reaction at a final concentration of 50 μ M. The reaction was allowed to proceed for 15 min. The reaction was then quenched with 20 mM EDTA and a final concentration of 2.5 mM *p*-nitrobenzyl mesylate (Abcam Biochemicals) was added and incubated for 2 h at room temperature. Phosphorylation was then probed using thiophosphate ester antibody RabMAb (ab92570) according to the manufacturer's protocol.

For Western blots, whole-cell extracts of *S. pombe* were made by flash freezing 2 O.D. of cells. Cells were then lysed in 100 μ l sample buffer (65 mM Tris, pH 6.8, 3% SDS, 10% glycerol, 10% 2-mercaptoethanol, 50 mM sodium fluoride, 50 mM β -glycerophosphate, 1 mM sodium orthovanadate, complete EDTA-free protease inhibitor tablet [Pierce]) in a Mini-beadbeater-16 for 2 min. Blots were probed with anti-FLAG M2 (Sigma), anti-GST (Covance), anti-Cdr1 (Opalko and Moseley, 2017), anti-Wee1 (Allard et al., 2018), anti-cdc2 (Santa Cruz Biotechnologies sc-53217), anti-pY15 (Cell Signaling #9111L), anti-His (Santa Cruz Biotechnologies sc-8036), and anti-thiophosphate ester (Abcam ab92570).

Mass spectrometry

Gel bands from Sf9 coexpression of Wee1 and Cdr1 and in vitro kinase assays were excised and destained overnight at 37°C using 50 mM ammonium bicarbonate/50% acetonitrile. The destained gel bands were protease-digested in 50 mM ammonium bicarbonate. To maximize sequence coverage, we tested three different proteases digestions: trypsin at 37°C for 16 h, GluC/LysC at 37°C for 16 h, or Proteinase K at 37°C for 1 h. In our initial mass spectrometry experiment, we found that Proteinase K provided the greatest sequence coverage, while trypsin and GluC/LysC were more limited (see Supplemental Table S2, Tab 3). For subsequent experiments, we used Proteinase K digestion, and three separate samples were tested in each condition. This approach dramatically increased our sequence coverage of Wee1. Following digestion, peptides were extracted using 5% formic acid/50% acetonitrile and dried. Peptides were analyzed on a Q-Exactive Plus mass spectrometer (Thermo Fisher Scientific) equipped with an Easy-nLC 1000 (Thermo Fisher Scientific). Raw data were searched using COMET in high-resolution mode (Eng et al., 2013) against the *S. pombe* sequence database, with appropriate enzyme specificity and carbamidomethylcysteine as static modification. Oxidized methionine and phosphorylated serine, threonine, and tyrosine were searched as variable modifications. We used a < 1% false discovery rate to filter the resulting peptide spectral matches. Quantification of LC-MS/MS spectra was performed using MassChroQ (Valot et al., 2011) with retention time alignment for smart quantification. Peak areas of Wee1 peptides were normalized to total amount of Wee1 in the sample. Probability of phosphorylation site localization was determined by phosphoRS (Taus et al., 2011). All Wee1 phosphorylation sites are provided in Supplemental Table S2. For the Wee1(K596L) experiment in Tab 2, we identified 12 sites only in the presence of Cdr1, 10 sites only in the absence of Cdr1, and six sites in both conditions. For the wild-type Wee1 experiment in Tab 4, we identified 35 sites

only in the presence of Cdr1, 12 sites only in the absence of Cdr1, and 18 sites in both conditions. For the in vitro kinase assays in Tab 5, we identified 41 sites only in the presence of active Cdr1, 50 sites only in the absence of active Cdr1, and 21 sites in both conditions. Combining all the sites from Tabs 2, 4, and 5, we identified 58 sites only in the presence of active Cdr1, 32 sites only in the absence of active Cdr1, and 47 sites in both conditions.

For phosphorylation sites identified by mass spectrometry, we generated a panel of nonphosphorylatable mutants (Ser to Ala), a subset of which are shown in Supplemental Figure S2C. We focused primarily on phosphorylated serines in the kinase domain because Cdr1 phosphorylates the Wee1 kinase domain alone and also preferentially phosphorylates serines (Coleman *et al.*, 1993; Parker *et al.*, 1993; Wu and Russell, 1993). Our initial mutagenesis targeted single sites, such as Ser771, that were highly phosphorylated in a Cdr1-dependent manner. All mutants were assayed for cell size at division, and most mutants were also tested by Western blot for changes in Wee1 phosphorylation and/or protein abundance in vivo. We focused on phosphosite mutants that changed cell size at division and Wee1 phospho-state, but did not influence Wee1 protein abundance and were nonadditive with *cdr1Δ*. Because *wee1(S771A)* caused a partial increase in cell size but did not abolish Wee1 phosphorylation in cells, we combined this mutant with nearby phosphosites in the predicted loop region, eventually leading to the *wee1(4A)* mutant.

Microscopy

Microscopy was performed at room temperature with a DeltaVision Imaging System (Applied Precision), equipped with an Olympus IX-71 inverted wide-field microscope, a Photometrics CoolSNAP HQ2 camera, and Insight solid-state illumination unit. All images are single focal plane images with a 5- μ m scale bar. Blankophor was used to identify septating cells for cell size measurements. ImageJ was used to measure cell length.

SWISS-MODEL and sequence alignment

The SWISS-MODEL was used to thread the kinase domain sequence of *S. pombe* Wee1 into the crystal structure of human Wee1 kinase domain (Guex *et al.*, 2009). The PyMOL Molecular Graphics system, Version 2.0 Schrödinger, LLC was used to visualize the model. For sequence alignments, clustal omega was used to align the Wee1 amino acid sequences from human and *S. pombe* Wee1 and *S. cerevisiae* Swe1 (Madeira *et al.*, 2019).

Statistics

All graphs and statistical analysis was performed using GraphPad Prism 8.0.2 (GraphPad Software, La Jolla, CA). A one-way analysis of variance (ANOVA) using Dunnett's multiple comparison test was used in Supplemental Figure S2C to compare each mutant strain to the wild-type control. A one-way ANOVA with Tukey's multiple comparison was used to compare more than two data sets.

ACKNOWLEDGMENTS

We thank Moseley lab members for comments and feedback, N. Ramirez and A. Grassetti for technical assistance, M. Sato for strains, and the Biomolecular Targeting Core (BioMT) (P20-GM113132) for equipment. This work was supported by grants from the American Cancer Society (RSG-15-140-01) and the National Institutes of Health/National Institute of General Medical Sciences (NIH/NIGMS) (R01GM099774) to J.B.M., by grants from the NIH/NIGMS (R35GM119455 P20GM113132) to A.N.K., and by a Norris Cotton Cancer Center support grant from the NIH/National Cancer Institute (P30CA023108).

REFERENCES

- Allard CAH, Opalko HE, Liu K-W, Medoh U, Moseley JB (2018). Cell size-dependent regulation of Wee1 localization by Cdr2 cortical nodes. *J Cell Biol* 217, 1589–1599.
- Allard CAH, Opalko HE, Moseley JB (2019). Stable Pom1 clusters form a glucose-modulated concentration gradient that regulates mitotic entry. *ELife* 8, e46003.
- Allen JJ, Manqing L, Brinkworth CS, Paulson JL, Wang D, Hübner A, Chou W-H, Davis RJ, Burlingame AL, Messing RO, *et al.* (2007). A semisynthetic epitope for kinase substrates. *Nat Methods* 4, 511–516.
- Aoi Y, Kawashima SA, Simanis V, Yamamoto M, Sato M (2014). Optimization of the analogue-sensitive Cdc2/Cdk1 mutant by in vivo selection eliminates physiological limitations to its use in cell cycle analysis. *Open Biol* 4, 140063.
- Breeding CS, Hudson J, Balasubramanian MK, Hemmingsen SM, Young PG, Gould KL (1998). The *cdr2(+)* gene encodes a regulator of G2/M progression and cytokinesis in *Schizosaccharomyces pombe*. *Mol Biol Cell* 9, 3399–3415.
- Coleman TR, Tang Z, Dunphy WG (1993). Negative regulation of the *wee1* protein kinase by direct action of the *nim1/cdr1* mitotic inducer. *Cell* 72, 919–929.
- Deminoff SJ, Ramachandran V, Herman PK (2009). Distal recognition sites in substrates are required for efficient phosphorylation by the cAMP-dependent protein kinase. *Genetics* 182, 529–539.
- Dunphy WG, Kumagai A (1991). The *cdc25* protein contains an intrinsic phosphatase activity. *Cell* 67, 189–196.
- Eng JK, Jahan TA, Hoopmann MR (2013). Comet: an open-source MS/MS sequence database search tool. *Proteomics* 13, 22–24.
- Featherstone C, Russell P (1991). Fission yeast p107wee1 mitotic inhibitor is a tyrosine/serine kinase. *Nature* 349, 808–811.
- Feilotter H, Nurse P, Young PG (1991). Genetic and molecular analysis of *cdr1/nim1* in *Schizosaccharomyces pombe*. *Genetics* 127, 309–318.
- Gautier J, Solomon MJ, Booher RN, Bazan JF, Kirschner MW (1991). *cdc25* is a specific tyrosine phosphatase that directly activates p34cdc2. *Cell* 67, 197–211.
- Gerganova V, Floderer C, Archetti A, Michon L, Carlini L, Reichler T, Manley S, Martin SG (2019). Multi-phosphorylation reaction and clustering tune Pom1 gradient mid-cell levels according to cell size. *ELife* 8, e45983.
- Gould KL, Nurse P (1989). Tyrosine phosphorylation of the fission yeast *cdc2+* protein kinase regulates entry into mitosis. *Nature* 342, 39–45.
- Guex N, Peitsch MC, Schwede T (2009). Automated comparative protein structure modeling with SWISS-MODEL and Swiss-PdbViewer: a historical perspective. *Electrophoresis* 30(Suppl 1), S162–S173.
- Hanks SK, Hunter T (1995). Protein kinases 6. The eukaryotic protein kinase superfamily: kinase (catalytic) domain structure and classification. *FASEB J Off Publ Fed Am Soc Exp Biol* 9, 576–596.
- Harvey SL, Charlet A, Haas W, Gygi SP, Kellogg DR (2005). Cdk1-dependent regulation of the mitotic inhibitor Wee1. *Cell* 122, 407–420.
- Hertz NT, Wang BT, Allen JJ, Zhang C, Dar AC, Burlingame AL, Shokat KM (2010). Chemical genetic approach for kinase-substrate mapping by covalent capture of thiophosphopeptides and analysis by mass spectrometry. *Curr Protoc Chem Biol* 2, 15–36.
- Kanoh J, Russell P (1998). The protein kinase Cdr2, related to Nim1/Cdr1 mitotic inducer, regulates the onset of mitosis in fission yeast. *Mol Biol Cell* 9, 3321–3334.
- Keaton MA, Lew DJ (2006). Eavesdropping on the cytoskeleton: progress and controversy in the yeast morphogenesis checkpoint. *Curr Opin Microbiol* 9, 540–546.
- Kellogg DR (2003). Wee1-dependent mechanisms required for coordination of cell growth and cell division. *J Cell Sci* 116, 4883–4890.
- Kim SY, Ferrell JE (2007). Substrate competition as a source of ultrasensitivity in the inactivation of Wee1. *Cell* 128, 1133–1145.
- Kumagai A, Dunphy WG (1991). The *cdc25* protein controls tyrosine dephosphorylation of the *cdc2* protein in a cell-free system. *Cell* 64, 903–914.
- Lu R, Niida H, Nakanishi M (2004). Human SAD1 kinase is involved in UV-induced DNA damage checkpoint function. *J Biol Chem* 279, 31164–31170.
- Lucena R, Alcaide-Gavilán M, Anastasia SD, Kellogg DR (2017). Wee1 and Cdc25 are controlled by conserved PP2A-dependent mechanisms in fission yeast. *Cell Cycle* 16, 428–435.
- Lundgren K, Walworth N, Booher R, Dembski M, Kirschner M, Beach D (1991). *mik1* and *wee1* cooperate in the inhibitory tyrosine phosphorylation of *cdc2*. *Cell* 64, 1111–1122.
- Madeira F, Park YM, Lee J, Buso N, Gur T, Madhusoodanan N, Basutkar P, Tivey ARN, Potter SC, Finn RD, *et al.* (2019). The EMBL-EBI search and

- sequence analysis tools APIs in 2019. *Nucleic Acids Res* 47, W636–W641.
- Martin SG, Berthelot-Grosjean M (2009). Polar gradients of the DYRK-family kinase Pom1 couple cell length with the cell cycle. *Nature* 459, 852–856.
- Moreno S, Klar A, Nurse P (1991). Molecular genetic analysis of fission yeast *Schizosaccharomyces pombe*. *Methods Enzymol* 194, 795–823.
- Morrell JL, Nichols CB, Gould KL (2004). The GIN4 family kinase, Cdr2p, acts independently of septins in fission yeast. *J Cell Sci* 117, 5293–5302.
- Moseley JB, Mayeux A, Paoletti A, Nurse P (2009). A spatial gradient coordinates cell size and mitotic entry in fission yeast. *Nature* 459, 857–860.
- Mueller PR, Coleman TR, Dunphy WG (1995). Cell cycle regulation of a *Xenopus* Wee1-like kinase. *Mol Biol Cell* 6, 119–134.
- Nurse P (1975). Genetic control of cell size at cell division in yeast. *Nature* 256, 547–551.
- Opalko HE, Moseley JB (2017). Dynamic regulation of Cdr1 kinase localization and phosphorylation during osmotic stress. *J Biol Chem* 292, 18457–18468.
- Pan KZ, Saunders TE, Flor-Parra I, Howard M, Chang F (2014). Cortical regulation of cell size by a sizer cdr2p. *ELife* 3, e02040.
- Parker LL, Atherton-Fessler S, Piwnicka-Worms H (1992). p107wee1 is a dual-specificity kinase that phosphorylates p34cdc2 on tyrosine 15. *Proc Natl Acad Sci USA* 89, 2917–2921.
- Parker LL, Walter SA, Young PG, Piwnicka-Worms H (1993). Phosphorylation and inactivation of the mitotic inhibitor Wee1 by the nim1/cdr1 kinase. *Nature* 363, 736–738.
- Pomerening JR, Sontag ED, Ferrell JE (2003). Building a cell cycle oscillator: hysteresis and bistability in the activation of Cdc2. *Nat Cell Biol* 5, 346–351.
- Russell P, Nurse P (1986). cdc25+ functions as an inducer in the mitotic control of fission yeast. *Cell* 45, 145–153.
- Russell P, Nurse P (1987). The mitotic inducer nim1+ functions in a regulatory network of protein kinase homologs controlling the initiation of mitosis. *Cell* 49, 569–576.
- Sakchaisri K, Asano S, Yu L-R, Shulewitz MJ, Park CJ, Park J-E, Cho Y-W, Veenstra TD, Thorner J, Lee KS (2004). Coupling morphogenesis to mitotic entry. *Proc Natl Acad Sci USA* 101, 4124–4129.
- Scheeff ED, Bourne PE (2005). Structural evolution of the protein kinase-like superfamily. *PLoS Comput Biol* 1, e49.
- Sha W, Moore J, Chen K, Lassaletta AD, Yi C-S, Tyson JJ, Sible JC (2003). Hysteresis drives cell-cycle transitions in *Xenopus laevis* egg extracts. *Proc Natl Acad Sci USA* 100, 975–980.
- Squire CJ, Dickson JM, Ivanovic I, Baker EN (2005). Structure and inhibition of the human cell cycle checkpoint kinase, Wee1A kinase: an atypical tyrosine kinase with a key role in CDK1 regulation. *Struct Lond Engl* 1993 13, 541–550.
- Strausfeld U, Labbé JC, Fesquet D, Cavadore JC, Picard A, Sadhu K, Russell P, Dorée M (1991). Dephosphorylation and activation of a p34cdc2/cyclin B complex in vitro by human CDC25 protein. *Nature* 351, 242–245.
- Taus T, Köcher T, Pichler P, Paschke C, Schmidt A, Henrich C, Mechtler K (2011). Universal and confident phosphorylation site localization using phosphoRS. *J Proteome Res* 10, 5354–5362.
- Taylor SS, Keshwani MM, Steichen JM, Kornev AP (2012). Evolution of the eukaryotic protein kinases as dynamic molecular switches. *Philos Trans R Soc Lond B Biol Sci* 367, 2517–2528.
- Valot B, Langella O, Nano E, Zivy M (2011). MassChroQ: a versatile tool for mass spectrometry quantification. *Proteomics* 11, 3572–3577.
- Wu L, Russell P (1993). Nim1 kinase promotes mitosis by inactivating Wee1 tyrosine kinase. *Nature* 363, 738–741.
- Young PG, Fantès PA (1987). *Schizosaccharomyces pombe* mutants affected in their division response to starvation. *J Cell Sci* 88, 295–304.